Chapter 2
Infrared and Ultraviolet Spectra of Fulleranes: HREELS Studies and Implications for the Interstellar Medium

Carlo Carraro[1], Roya Maboudian[1], and Conrad R. Stoldt[2]

Abstract The reaction of atomic hydrogen with few-layer buckminsterfullerene films deposited on silicon in ultrahigh vacuum produces fullerane mixtures, which are studied in situ by high resolution electron energy loss spectroscopy. The vibrational and electronic excitation spectra are measured and discussed. Their main features are compared to observational data, including the infrared emission from interstellar and circumstellar clouds and the interstellar extinction curve. Laboratory spectra show remarkable agreement with important features detected in the observational data, among others the so-called canonical interstellar spacing of infrared spectra and the single bump in the ultraviolet absorption spectra. These studies suggest that members of the buckminsterfullerane family may be the primary carriers of the unidentified spectral features seen in interstellar dust.

2.1 Introduction

Various forms of molecular carbon, from ions to radicals, have been detected in the diffuse interstellar medium (ISM) using electronic, rotational, and vibrational spectroscopies (Henning and Salama 1998; Snow and Witt 1995). Discrete absorption and emission bands seen toward diffuse interstellar clouds indicate the presence of numerous two-atom molecules such as CO, CN and C_2. In addition to these interstellar features, a large family of spectral bands observed from the far-UV to the far-IR still defies explanation. Currently, it is the general consensus that many of the unidentified spectral features are formed by a complex, carbonaceous species that show rich chemistry in interstellar dust clouds (Ehrenfreund

[1]Department of Chemical Engineering, University of California, 201 Gilman Hall, Berkeley, CA 94720-1462, USA
e-mail: carraro@berkeley.edu; maboudia@berkeley.edu

[2]Department of Mechanical Engineering, University of Colorado, Boulder, CO 80309-0427, USA
e-mail: conrad.stoldt@colorado.edu

F. Cataldo and S. Iglesias-Groth (eds.), *Fulleranes: The Hydrogenated Fullerenes*, Carbon Materials: Chemistry and Physics 2, DOI 10.1007/978-1-4020-9887-1_2,

and Charnley 2000). Such species are likely to not consist entirely of carbon, as the ubiquitous presence of hydrogen in the interstellar medium suggests that some degree of hydrogenation should be expected. The presence of an unidentified infrared emission (Gillett et al. 1973) and the evidence of adsorption near 2,900 cm^{-1} in the line of sight to the galactic center (Soifer et al. 1976), typical of CH stretching vibrations, lend observational support to this expectation. Potential candidates include polycyclic aromatic hydrocarbons, hydrogenated amorphous carbon and fulleranes.

Here, we summarize our laboratory studies of mixtures of hydrides of buckminsterfullerene, prepared by reaction of C_{60} films with an atomic hydrogen flux in ultrahigh vacuum (UHV), and analyzed by means of High Resolution Electron Energy Loss Spectroscopy (HREELS). These studies afford us a broad window of energy loss, spanning from the infrared to the ultraviolet. A precise assessment of the degree of hydrogenation of the films is not conducted, in part because of the sheer difficulty of the task, but also because of the questionable usefulness of such assessment, vis-a-vis the variability expected in the degree of hydrogenation of carbonaceous species in various interstellar conditions. A theoretical analysis by Webster (1992a) suggests that the degree of hydrogenation results from the equilibrium between ultraviolet flux, which promotes hydrogen photodetachment, and interstellar gas density, which promotes attachment. Thus, a varying degree of hydrogenation will follow, among other factors, from variable environmental harshness.

2.2 The Unidentified Infrared Emission Problem

The term "unidentified infrared emission" is used to refer to the long-known emission features of interstellar dusts in the spectral region from just over 3,000 cm^{-1} to below 800 cm^{-1} (Gillett et al. 1973). These features comprise sharp IR bands at 2,920, 1,610, and 880 cm^{-1}, as well as a broader envelope near 1,300 cm^{-1}. In addition, a recurrent mode at 3,050 cm^{-1}, a weak mode near 1,450 cm^{-1}, and a shoulder near 1,150 cm^{-1} are observed. These spectral features can all be attributed to vibrational modes of hydrogenated carbon species, as summarized in Table 2.1. The chemical structure of these species remains the subject of debate. Furthermore, a number of carbon-rich astronomical objects reveal an emission feature in the far-IR at 490 cm^{-1}, of unclear attribution (Kwok et al. 1989).

Any hydrogenated candidate for the unknown IR emission must exhibit sufficient stability to the harsh conditions of the interstellar medium, including bombardment by particles and ultraviolet and gamma radiation. Equally important, for a species to be considered a viable candidate, its spectra must reproduce two important characteristics found in most diffuse medium spectra. These are (a) that the 1,300 cm^{-1} band be more intense than the 880 cm^{-1} band (Williams 1996), and (b) that the spacing between it and the next main emission feature match the "canonical interstellar spacing" of 300 cm^{-1} (Hudgins and Allamandola 1999).

2.3 The Ultraviolet Extinction Curve

From far-UV to near-IR wavelengths, diffuse ISM spectra exhibit a smooth continuum known as the interstellar extinction curve. The most prominent unidentified spectral feature on this curve is the so-called UV absorption bump at 217 nm. Characterized by a constant position and a bandwidth that varies with interstellar conditions (Fitzpatrick and Massa 1986), this feature is believed to result from electronic π–π^* interband transitions in hydrogen containing carbonaceous dust (Henning and Salama 1998). Most theoretical approaches adopt a small, spherical or spheroidal form of graphite as the candidate for the UV bump carrier (Mathis 1996), although most models indicate that the electronic structure of graphite must be modified to satisfy observational constraints (Li and Greenberg 1997). Below the bump, a number of weak, diffuse interstellar bands (DIBs) are detected on the continuum between 400 and 1,200 nm. The nature of the DIBs is still in question, although their narrow linewidths suggest unresolved rotational and vibrational structure from electronic excitations in gas-phase, organic molecules (Herbig 1995; Sarre et al. 1995). The strongest and broadest DIB, found at 443 nm, exhibits a nonvariable wavelength and weakens in dense interstellar clouds, as do all of the DIBs and the UV absorption bump.

The discovery of C_{60} by Kroto and coworkers (1985) was motivated in part by the interstellar dust problem. C_{60} would seem to be an ideal candidate, as it is spherical and graphite-like, it forms spontaneously in harsh environments with carbon dust, and is stable in intense radiation fields, a condition analogous to that found in the diffuse ISM (Kroto and Jura 1992). In fact, the observation of two DIBs at 957.7 and 963.2 nm are tentatively considered the first evidence of C_{60}^+ in interstellar dust (Foing and Ehrenfreund 1997). Moreover, a mixture of hydrides of C_{60} is shown to exhibit spectral features remarkably similar to those seen in the unidentified infrared emission (Stoldt et al. 2001). The UV absorption spectrum of synthetic $C_{60}H_{36}$ was also observed to possess a broad bump at 217.5 nm (Cataldo 2003).

2.4 Experimental Procedures

The C_{60} films described below were prepared in UHV on (2 × 1) reconstructed Si(100) substrates. C_{60} is evaporated from a Knudsen cell held at 410°C for approximately 10 min, yielding a reddish brown multilayer (>10 layer thick) film. A mixture of hydrides of buckminsterfullerene was prepared via the interaction of atomic hydrogen with the uppermost layers of the deposited C_{60} film at 25°C. Atomic hydrogen was generated by the dissociation of H_2 at a spiral tungsten filament heated to 1,600°C (hydrogen exposures are given in terms of molecular hydrogen and reported in Langmuirs (1 Langmuir (L) ≡ 10^{-6} Torr · s). These exposures correspond to a flux of roughly 3×10^{13} hydrogen atoms/(cm^2·langmuir) at the sample surface.

High-resolution electron energy loss spectra were obtained using an LK Technologies model ELS3000 spectrometer. In this technique, an energetic electron beam impinges on a surface and electrons scattered into a given detection angle (in the specular direction, unless otherwise noted) are energy analyzed. For spectra acquisition in the IR region, the primary electron beam energy is 6 eV, at an incident angle of 60° toward the surface normal, with resolution set at 3 meV. For the ultraviolet-visible region, the beam energy is varied between 18 and 50 eV and the instrumental energy resolution is set to 28 meV. The sample temperature is held at −150°C during spectra acquisition. The reader must note that HREELS differs in several important aspects from optical spectroscopies. In particular, the excitation mechanism has two components, one electromagnetic (electric dipole scattering) and one short range (impact scattering). Thus, HREELS spectra are somewhat richer (and more complex) than optical spectra, and usually reveal features that can be observed only by a combination of other techniques (e.g., IR, Raman, and neutron scattering).

2.5 Results

2.5.1 Infrared Spectra

The effect of hydrogen exposure on the vibrational spectrum of fulleranes $C_{60}H_x$ is reported by Stoldt et al. (2001). The results are summarized in Fig. 2.1. The vibrational spectrum of C_{60} is displayed in plot (*a*), while plots (*b*)–(*d*) illustrate the effects of increasing doses of hydrogen exposure. New loss features appear upon hydrogen exposure. C-H stretch vibration modes are detected as an intense peak centered at 2,900 cm^{-1}. Furthermore, a broad band develops between 1,425 and 1,060 cm^{-1}, and two smaller bands appear near 2,490 and 1,620 cm^{-1}. Additional peaks grow in intensity at 880 and 480 cm^{-1}, while the intensities of the peaks at 765 and 525 cm^{-1} begin to decline with increasing exposure to hydrogen flux. A number of loss peaks are not associated with observed astronomical spectral features, as discussed in the original report. The peaks at 765, 575, and 525 cm^{-1} are clearly due to vibrational modes of the unexposed C_{60} multilayer beneath the uppermost hydrogenated layer(s). To support this conclusion, off-specular HREEL spectra were obtained. In this geometry, scattering is mainly due to the impact mechanism. This allows one to suppress the effect of long range excitation, and thus, the signal resulting from deep buried layers. The off-specular data also reveals that the 1,220 cm^{-1} mode is not dipole excited and hence, it should not be prominent in IR emission spectra. Likewise, the mode centered at 2,490 cm^{-1}, attributable to a multiple loss (the sum of the modes between 1,450 and 1,150 cm^{-1}), will not appear in an optical spectrum. The remaining loss features found in the spectra of Fig. 2.1, plots (b–d), i.e., the losses measured at 2,900, 1,620, 1,425, 1,310, 1,150, and 880 cm^{-1}, compare favorably both with theoretical calculations and with observational evidence. In particular, note that the HREEL spectra shown in Fig. 2.1, plots (b–d),

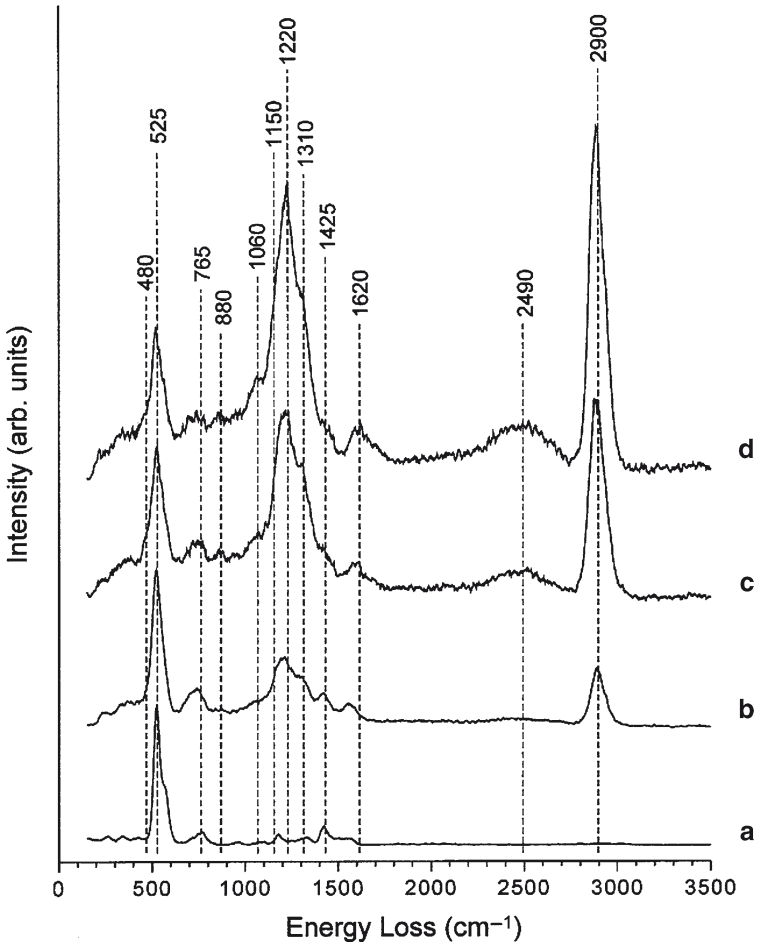

Fig. 2.1 HREEL spectra of C_{60} multilayer films shown as a function of increasing hydrogen exposure. The primary electron beam energy is 6 eV and the sample temperature is −150°C. (**a**) no hydrogen exposure, FWHM = 36.5 cm^{-1}; (**b**) a 45 L hydrogen exposure, FWHM = 34.8 cm^{-1}; (**c**) a 180 L hydrogen exposure, FWHM = 40.4 cm^{-1}; and (**d**) a 1,000 L hydrogen exposure, FWHM = 60.4 cm^{-1}. Spectral features labeled for comparison with Table 2.1 (Reproduced by permission of the AAS from Stoldt et al. 2001).

satisfy both spectral prerequisites mentioned above (canonical interstellar spacing and relative intensity of the 1,310 cm^{-1} band). In this regard, the observation that the position of the 1,310 cm^{-1} band does not shift with degree of hydrogenation is particularly significant, as it lends support to the hypothesis that an admixture of buckminsterfulleranes with broad (and varying) degree of hydrogenation may be responsible for the unidentified emission. Overall, the experimental losses featured in Fig. 2.1 (b–d) and attributable to buckminsterfullerane species are comparable in wavelength to the unidentified IR emission features listed in Table 2.1.

Table 2.1 Unidentified astronomical IR emission frequencies and their typical assignments

Astronomical frequency (wave numbers)	Typical mode assignment
3,050	sp^2 aromatic C–H stretch
2,800–3,000	sp^3 aliphatic C–H stretch
1,620	Aromatic C–C stretch
1,450	Aromatic C–C stretch, aliphatic C–H deformation
1,250–1,300	Blending of aromatic C–C stretch bands
1,150	Aromatic C–H in-plane bend
1,050–1,810	Blending of several weak aromatic C–C stretch bands
885	Aromatic C–H out-of-plane bend
490	Unknown

Lastly, two additional comments are in order. One concerns the shoulder that is seen to grow in intensity with hydrogen exposure near 480 cm^{-1}. This frequency, close to the calculated $2F_{1u}$ normal mode of $C_{60}H_{60}$, is nearly the same frequency of an "unidentified" mode recurring in observations of carbon-rich astronomical objects, and discussed previously. The second comment concerns the identity of the carrier of the IR emission line at 3050 cm^{-1}, an aromatic C–H strech, whose origin was attributed by Webster (1991) to lightly hydrogenated fullerane such as $C_{60}H$ or $C_{60}H_2$. Here, we note that for low hydrogen exposures, HREEL spectra show a broad band centered at 2,900 cm^{-1} and extending up to only 3,000 cm^{-1}. Only with exposures in excess of 2,000 L is the formation of aliphatic CH_2 and CH_3 bending modes detected in HREEL spectra. This observation was interpreted as suggesting that bond cleavage occurs after extended hydrogen bombardment, with generation of hydrogenated aromatic fragments from the broken up C_{60} cage, a likely occurrence also during extensive exposure to atomic hydrogen in the diffuse medium.

2.5.2 Ultraviolet Spectra

The far-UV to near-IR EEL spectrum of the unexposed C_{60} film is exhibited in Fig. 2.2a, in close agreement with spectra reported previously for thick C_{60} films on Si(100) (Gensterblum 1991). The characteristic "camel back" features, which exclude C_{60} as a carrier of the interstellar extinction, are readily observed at 195 and 260 nm. The three peaks at 260, 335 and 420 nm are seen in absorption spectroscopy (AS), and correspond to dipole-allowed, ^1A_g–$^1T_{1u}$, single-electron π–π^* transitions in the C_{60} molecule (Leach 1992; Hare et al. 1991). The intense peak at 195 nm is the so-called π-plasmon that results from a collective excitation of the molecular π-electron subsystem. The collective nature of this excitation is affirmed by our experimental observation that its intensity is variable upon changing the primary electron energy of the EEL spectrometer (Lucas 1992). Additionally, this band is broadened and blue-shifted when compared to the narrower transition seen in AS

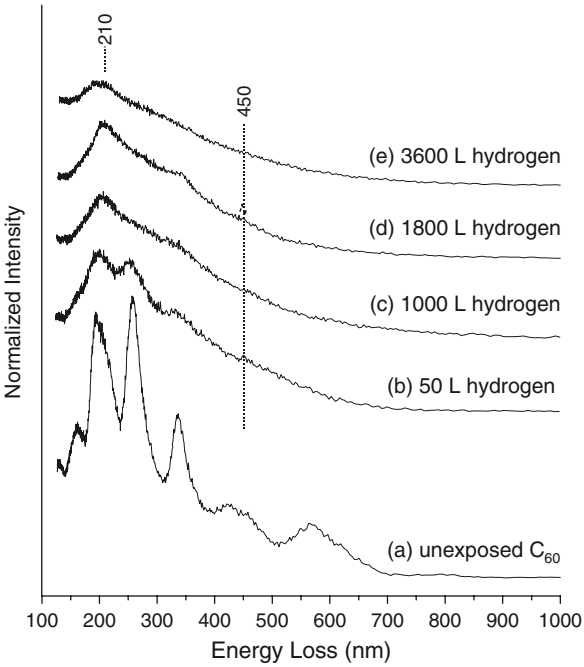

Fig. 2.2 EEL spectra of C_{60} multilayer films shown as a function of increasing hydrogen exposure. The primary electron beam energy is 50 eV and the sample temperature is −150°C. The FWHM of the individual spectra are (**a**) 44.8, (**b**) 34.4, (**c**) 33.1, (**d**) 40.7, and (**e**) 37.2 meV

near 210 nm, owing to the modified response function pertinent to the reflection geometry of EELS experiments.

Looking now at the hydrogenated C_{60} spectra shown in Fig. 2.2b–e, a number of distinct spectral changes are seen. The most significant is the observation of an intense, broad loss peak near 210 nm with low to moderate hydrogen exposure (Fig. 2.2b–d). This strong band is positioned between the two peaks which give the C_{60} spectrum its "camel back" character. The intensity of this loss peak is observed to vary with primary electron energy, indicating that it is associated with excitations of the π-electron system. Further hydrogenation of the C_{60} film results in a decrease in intensity of the 210 nm band, as seen in Fig. 2.2e. The π-plasmon, initially at 195 nm, is observed to shift to 210 nm and decrease in intensity with increasing hydrogen exposure. The astronomical UV bump shows a similar pattern of variability: the intensity is low in dense gas and high in the opposite conditions. As mentioned previously, this mode is blue-shifted in EELS and is detected closer to 220 nm in AS. Also observed is a small loss shoulder near 450 nm in the spectra of Fig. 2.2b–d that loses intensity with increasing hydrogen exposure. The broadest DIB, observed at 443 nm, behaves similarly in that it is most intense in more diffuse interstellar clouds.

The source of the 210 nm UV band in our spectra of partially hydrogenated C_{60} is now discussed in the context of a theory previously detailed by Webster (1992b, 1993a). In Fig. 2.2a, the π-plasmon of unhydrogenated C_{60} yields an intense loss peak near 190 nm that is attributed to the collective oscillations of the global π-electron system. With extended hydrogen exposure, every hydrogen atom that is attached to C_{60} results in the loss of a single π-electron and as a consequence, the spatial extent to which the molecule is conjugated decreases as well. In other words, the global π-electron system is broken up into several isolated local systems surrounded by hydrogen-bearing carbon atoms. When fully hydrogenated, the C_{60} molecule is aliphatic, and will exhibit no π-plasmon (or UV bump). The small local π-systems that remain embedded in C_{60} following prolonged hydrogen exposure have known analogs in molecules such as benzene, and in small odd-alternant radicals such as C_3H_5. Such molecules are known to have transitions at UV or visible wavelengths that may contribute to the astronomical UV absorption bump and the DIBs (Webster 1993b).

A complication that arises with this analysis concerns the nearly 10^{15} possible isomers of hydrogenated C_{60} which will each yield a unique electronic spectrum. Astronomical observations show systematic behavior in the spectra of diffuse molecular clouds (Mathis 1990), suggesting that the dynamic equilibrium which exists between competing astrophysical processes will favor certain molecular species depending on the interstellar environment. As a result, the enormous number of isomers of hydrogenated C_{60} may be significantly reduced to a few stable hydride families having 'magic numbers' of hydrogen atoms favored by symmetry considerations (Webster 1993a). This conjecture is supported by our previous observation that the vibrational spectra of a mixture of hydrides of C_{60} only exhibit the "canonical interstellar spacing" of 300 cm^{-1} after prolonged hydrogen exposure (Stoldt et al. 2001). Low degrees of hydrogenation do not satisfy this requirement of astronomical spectra, indicating that the interstellar environment selects higher hydrides of C_{60}.

In Fig. 2.3a, the EEL spectra of clean and hydrogenated C_{60} are compared with the variable component of the interstellar extinction curve. The two-component model for the interstellar extinction (Webster 1997) has a nonvariable or ubiquitous component attributed to classical-sized dust grains, and a variable component (shown in Fig. 2.3a) which is connected with hydrogenated carbonaceous molecules. The visible spectrum of hydrogenated C_{60} shows good agreement with the variable extinction curve, in particular reproducing the distinct kink near 500 nm, while the EEL spectrum of C_{60} does not. In Fig. 2.3b, the EEL spectrum of hydrogenated C_{60} is compared to the mean interstellar extinction curve. The structure of the two curves is similar: each shows a far-UV extinction at short wavelengths below 200 nm; a strong UV bump between 210 and 220 nm; and a near-featureless extinction from the near-UV to the near-IR.

The main discrepancy between the two curves in Fig. 2.3b is the strong loss shoulder due to the dipole-allowed transitions of C_{60} at 260 and 335 nm in the hydrogenated C_{60} EEL spectrum. Adding hydrogen to C_{60} will reduce the symmetry or eliminate it entirely, simultaneously decreasing the intensity of these transitions. In Fig. 2.2b–e, extended hydrogen exposure does lead to a reduction in the intensity

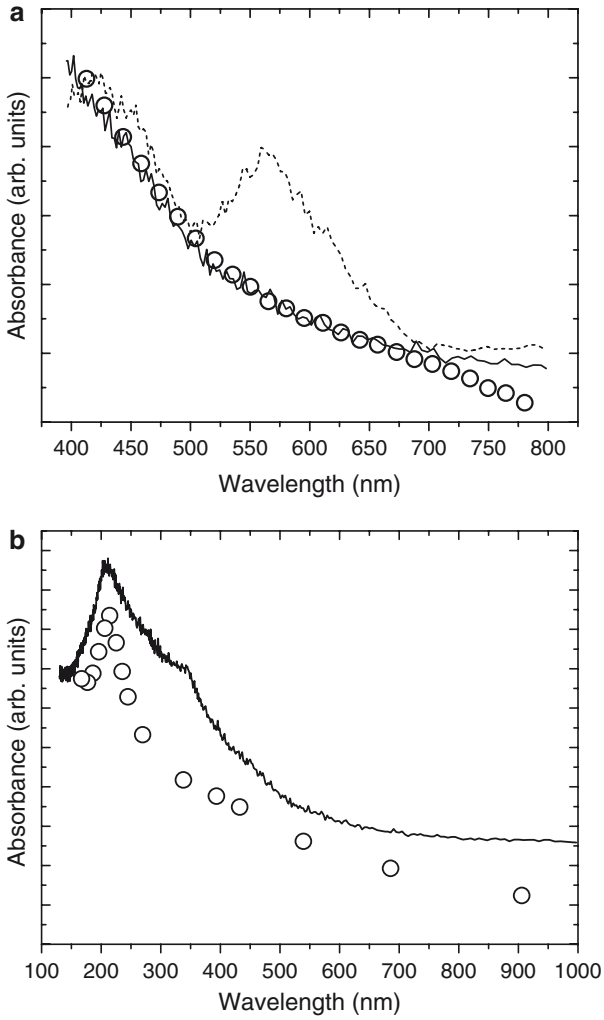

Fig. 2.3 (a) The visible-band EEL spectra of unexposed (*dashed line*) and hydrogenated (*solid line*) C_{60} films shown in Fig. 2.2, spectra labeled (a) and (d), compared with the extinction curve of the variable component (open circles) detailed in Webster (1997). (b) The far-UV to near-IR EEL spectrum of the hydrogenated C_{60} film (*solid line*) in Fig. 2.2 (d) compared to the mean interstellar extinction curve (*open circles*). The vertical scales of the EEL spectra and extinction curves in Fig. 2a and b are incommensurable, and the EEL spectra are arbitrarily scaled to give reasonable qualitative agreement for comparison

of these bands, although they are not entirely removed. By performing experiments on a monolayer C_{60} film, we have confirmed that some contribution to these bands results from excitations of the underlying C_{60} layers which remain not hydrogenated. A second contribution may result from the random nature of energetic hydrogen bombardment, which will yield a wide degree of hydrogenation in any one

HREELS experiment. This should result in some amount of lightly hydrogenated C_{60} molecules in the uppermost layer of the film. Interestingly, the UV-visible spectra of $C_{60}H_2$ and $C_{60}H_4$ (Webster 1993b) are very similar to that of clean C_{60} in regard to the strength of the dipole-allowed transitions, indicating that the addition of a small number of hydrogen atoms does not sufficiently perturb the molecule's electronic structure. Therefore, a wide degree of hydrogenation may be the source of the strong transitions characteristic of pure C_{60} in the hydrogenated films, perhaps intensified by a contribution from optically inactive impact scattering modes. We can also infer that interstellar C_{60} must exhibit both a high average degree of hydrogenation (at least more than four hydrogens) and a smaller range of hydrides lending further support to the 'magic number' scenario.

2.6 Conclusions

Mixtures of fulleranes produced by hydrogenation of solid C_{60} films under atomic H flux have revealed spectral features that bear striking similarity to those observed in the diffuse interstellar medium, both in the far IR and in the UV spectral windows. Of course, one must be cautious not to overextend the interpretation of laboratory data, for a number of reasons: firstly, because electron spectroscopy, the experimental technique used in these studies, differs in several important aspects from the spectroscopic methods employed in observational astronomy, and secondly, because of the specifics of specimen preparation and environmental conditions. In this regard, there is a need to explore the stability of fulleranes to energetic and corpuscular radiation (Cataldo et al. 2009). Nonetheless, our findings lend support to the suggestion of fulleranes as candidates for unidentified emission and absorption features of interstellar and circumstellar media. Whether or not they exist in sufficient abundance is still unclear; however, their spectral features make them undoubtedly an ideal model system for laboratory studies of these fascinating astrophysical phenomena.

References

Cataldo F (2003) Fullerenes Nanotubes Carbon Nanostructure 11:295
Cataldo F, Strazzulla G, Iglesias-Groth S (2009) MNRAS 394:615
Ehrenfreund P, Charnley SB (2000) Annu Rev Astron Astrophys 38:427
Fitzpatrick EL, Massa D (1986) Astrophys J 307:286
Foing BH, Ehrenfreund P (1997) Astron Astrophys 317:L59
Gensterblum G (1991) Phys Rev Lett 67:2171
Gillett FG, Forrest WJ, Merrill KM (1973) Astrophys J 183:87
Hare JP, Kroto HW, Taylor R (1991) Chem Phys Lett 177:394
Henning T, Salama F (1998) Science 282:2204
Herbig GH (1995) Annu Rev Astron Astrophys 33:19

Hudgins DM, Allamandola LJ (1999) Astrophys J 513:L69
Kroto HW, Jura M (1992) Astron Astrophys 263:275
Kroto HW, Heath JR, O'Brien SC, Curl RF, Smalley RE (1985) Nature 318:162
Kwok S, Volk K, Hrivnak BJ (1989) Astrophys J 345:L51
Leach S (1992) Chem Phys 160:451
Li A, Greenberg JM (1997) Astron Astrophys 323:566
Lucas AA (1992) J Phys Chem Solids 53:1415
Mathis JS (1990) Annu Rev Astron Astrophys 28:37
Mathis JS (1996) Astrophys J 472:643
Sarre PJ, Miles JR, Scarrott SM (1995) Science 269:674
Snow TP, Witt AN (1995) Science 270:1455
Soifer BT, Russell RW, Merrill KM (1976) Astrophys J 207:L83
Stoldt CR, Maboudian R, Carraro C (2001) Astrophys J 548:L225
Webster A (1991) Nature 352:412
Webster AS (1992a) Astron Astrophys 257:750
Webster A (1992b) MNRAS 255:41
Webster A (1993a) MNRAS 263:385
Webster A (1993b) MNRAS 265:421
Webster A (1997) MNRAS 288:221
Williams DA (1996) Astrophys Space Sci 237:243

http://www.springer.com/978-1-4020-9886-4

Fulleranes
The Hydrogenated Fullerenes
Cataldo, F.; Iglesias-Groth, S. (Eds.)
2010, XIV, 350 p., Hardcover
ISBN: 978-1-4020-9886-4